lished results), and ligated into Sac I–cleaved pFRC1P (that is, at a site adjacent to that of the inserted *xylS* gene), to obtain plasmid pFRC3P. Finally, a 7.3-kb fragment that contained the *xylXYZLS* genes was excised from pFRC3P by cleavage with Hind III and partial cleavage with Eco RI; the sticky ends were filled in with the Klenow fragment of DNA polymerase I, and the fragment was cloned into the Sma I site located in the Tn*5* transposon present on the narrow host range transposon donor plasmid pSUP2021 (*18*). The resulting hybrid plasmid, designated pFRC4P, was mobilized into B13 in a triparental mating that involved B13 as recipient, *E. coli* HB101 (pFRC4P) as donor, and *E. coli* HB101 (pRK2013) (*19*) as helper. Kanamycin-resistant derivatives of B13 were selected in which the Tn*5* hybrid transposon that carried the cloned TOL genes had transposed into the chromosome.

17. C. Yamisch-Perron, J. Viera, J. Messing, *Gene* **33**, 103 (1985).
18. R. Simon, U. Priefer, A. Pühler, *Biotechnology* **1**, 784 (1983).
19. M. Kahn *et al.*, *Methods Enzymol.* **68**, 268 (1980).
20. D. H. Pieper, K.-H. Engesser, R. H. Don, K. N. Timmis, H.-J. Knackmuss, *FEMS Microbiol. Lett.* **29**, 63 (1985).
21. H. W. Boyer and D. Roulland-Dussoix, *J. Mol. Biol.* **41**, 459 (1969).
22. H.-J. Knackmuss and M. Hellwig, *Arch. Microbiol.* **117**, 1 (1978).

23. We thank J. L. Ramos, S. Harayama, D. F. Dwyer, and B. Staskawicz for bacterial strains and stimulating discussions, and F. Rey for expert secretarial assistance. We also thank the Bunderministerium für Forschung und Technologie, Bonn, for supporting part of this work, and the European Molecular Biology Organization for providing a long-term postdoctoral fellowship to one of us (F.R.).

22 June 1987; accepted 22 September 1987

Fluvial Perturbance in the Western Amazon Basin: Regulation by Long-Term Sub-Andean Tectonics

MATTI E. RÄSÄNEN, JUKKA S. SALO, RISTO J. KALLIOLA

Haffer's refuge theory proposes that during the arid climatic phases of the late Pleistocene, tropical lowland forests of Amazonia were reduced to isolated patches contributing to the high species richness of the present-day forest. The theory was developed because no obvious historic or modern geomorphic isolation barriers were recorded in Amazonia. Analyses of radar images combined with stratigraphical data show that in the basinal forelands of the tectonically active Andes the geological setting causes long-term fluvial perturbance. This leads to a temporally structured highly complex mosaic of fossil and present floodplains. These dynamics have been present with varying activity and geographic range during the Tertiary and Quaternary, providing site-turnover that has not been recognized by the biogeographic tradition of the Amazon basin.

THOUGH THE CLIMATIC REFUGE theory (*1*) has dominated the recent biogeography of Amazonia, there are still no undisputed litho- or biostratigraphic or geomorphologic data to show that the Amazon lowland forest (<500 m above sea level) has fragmented to isolated patches during the Pleistocene. The biogeographic works limiting "refuges" as centers for high endemism or species diversity (*2, 3*) fail to present geologic evidence that these locations have been separated by savanna vegetation (*4*). On the other hand, Liu and Colinvaux (*5*) have shown that during the mid-Wisconsin interstade, the Mera site (1100 m above sea level) in the proposed Napo refuge area in Ecuador (*3*) was not covered by tropical broad-leaved lowland forest but rather by *Podocarpus*-dominated Andean montane forest. This suggests that during the full-glacial times of the Pleistocene, the lowland broad-leaved forest merely decreased in area but did not fragment.

A new approach to species diversity dynamics, based on the mosaic forest bed structure and maintained by fluvial perturbance of western Amazonia, has recently been put forward (*6*). Campbell and Frailey alternatively suggested that the whole forest bed of western Amazonia is formed by Holocene alluvium, promoting a forest community "island" in a stage of supersaturated disequilibrium (*7*). Colinvaux *et al.* (*8*) have proposed that the high species diversity of the floodplains of the Napo and Aguarico rivers is maintained by hydraulic disturbance, especially catastrophic floods, which cause intermediate disturbance in the floodplain forests.

We present further evidence that besides the Tertiary-Quaternary climatic fluctuation, and shifting between marine and continental phases, western Amazonia has been subjected to fluvial site-turnover processes similar to present floodplain dynamics. On present floodplains, channel migration and sedimentation maintain high between-habitat (β-type) diversity through packing forest patches of different age close to each other. Channel diversions of the aggrading rivers cause floodplain alterations and subsequent larger scale areal mosaicism. Finally, larger geomorphic barriers are formed within the lowland forest by the foreland basins, separated by distinctive upper denudated areas.

Western Amazonia (Fig. 1) forms part of the foreland molasse basin belt running along the eastern foothills of the Andes (*9, 10*) and the Rocky Mountains in North America. It is located between the positively epeirogenic Guayanan-Brasilian craton (*11, 12*) and the Andean mountain range with postorogenic uplift. The area is subject to compressive crustal shortening and can be characterized as a thin-skinned fold and thrust belt (*13–16*). Among the most similar present-day environments is the Indogangetic plain with the Bengal basin, drained by the Ganges and Brahmaputra rivers along the Himalayas (*17*).

The present structural system of western Amazonia includes four major foreland ba-

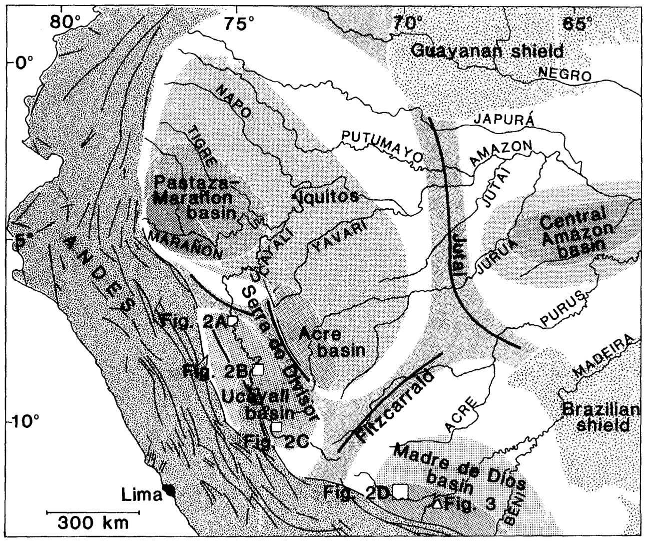

Fig. 1. The major geological structures in the western Amazonia [modified after (*9, 11, 12, 14, 18, 19*)]. The molasse basins of Pastaza-Marañon, Ucayali, Madre de Díos, and Acre are separated by arches. The relative vertical extent of Tertiary-Quaternary deposits in the central parts of the lowland basins is depicted by the intensity of dotting. The Andes are characterized by fault lines (*9*) and the positions of the reverse faults on the eastern side of the anticlines of the sub-Andean fault system are shown (*14–16*). The four areas analyzed in Fig. 2 are marked by squares. The site of Fig. 3 is shown by a triangle.

M. E. Räsänen, Department of Quaternary Geology, University of Turku, SF-20500 Turku, Finland.
J. S. Salo and R. J. Kalliola, Department of Biology, University of Turku, SF-20500 Turku, Finland.

sins (Fig. 1) (*11, 12, 18, 19*). The geologic evolution of these basins is regulated by the sub-Andean fault system, running along the eastern side of the Andes (*14–16*). The present-day pattern, with a miogeosyncline on the eastern side of the emerging mountain chain, was reached in the late Mesozoic (*10, 14, 16, 20*). The basins and a major part of the fault system originated time-transgressively (in phases from west to east) from the late Permian to the Quaternary (*14–16*). Since the Cretaceous, the sediments in the basins have been mostly continental fluvial deposits. The infilling of these miogeosynclinal basins was mainly with riverine sediments from the shield areas in the east. Marine transgressions from the west have caused shifting of marine-deltaic-floodplain environments with marine dominance in the west (*16, 19, 21*).

The widely distributed "red beds" (*22*) were deposited in the basinal areas during the Tertiary Andean orogenies and they show dominance of continental deposits originating increasingly from the west (*23, 24*). In the Pastaza-Marañon and Ucayali basins the sedimentation was intercalated by marine intrusion during the early Oligocene (Pozo Formation) (*25*). Later during the Neogene, contemporarily with the latest orogeny of the Andes, a brackish or freshwater lake formed in the Pastaza-Marañon and Acre basins (Pebas Formation) (*26*) and because of the continuing uplift the easterly course of the Amazon river was created (*27*). The Cretaceous-Tertiary development led to total aggradation of 4 to 11 km of deposits in the subsiding basins (*9*).

Today, the Pastaza-Marañon and Ucayali basins have distinct central areas of subsidence and accumulation of fluvial sediments (*28*). The Quaternary molasse sediments in the subsiding basins are of great vertical extent: the Corrientes Formation in the Pastaza-Marañon basin reaches 1500 m (*29*), the corresponding Quaternary counterparts of the Ica and Solimões formations at Acre probably have great depth (*25*). This vertical extent reflects active Andean uplift and erosion in the Quaternary. The present areas of subsidence or accumulation are characterized by riverine geomorphic structures (Fig. 2A). However, the extent of these areas has varied during the Quaternary. Shifting tectonic and climatic events have affected the balance of sedimentation and the compensating isostatic, tectonic, or compaction-induced subsidence in the areas of accumulation.

The basins are surrounded by anticlinal emerging arches (Fig. 1) (*11, 14*). Higher lying areas along the arches and margins of the basins are widely covered by Quaternary fluvial deposits and are nowadays subject to denudation and downcutting of even the smallest tributaries. This suggests the recent uplift of the areas (*11, 24, 30*) or alternatively a decrease in sedimentation after the Pleistocene glacial phases (*11, 31*).

Figure 2 illustrates the deposition-erosion continuum from *várzea* (flooded) to *tierra firme* (nonflooded) forest bed, as evidenced by four selected sites in Peruvian Amazonia. The geomorphology reveals well-preserved evidence of probably tectonically induced floodplain dynamics over a much wider area than previously reported (especially Fig. 2D) (*32*) and suggests them to be of Pleistocene-Holocene age. In addition to the unidirectional sequential migration of floodplains (Fig. 2D), the impact of tectonics is evidenced by the tilting of drainage networks of floodplains in the Acre and Ucayali basins (*6, 11*). The cyclothemic stratigraphy of the Pleistocene-Holocene floodplain deposits, which widely form the present *tierra firme* level in the western Amazon lowlands (Fig. 3) (*24, 33*), must be interpreted as a result of both autocyclic and allocyclic control (*34*) with major influence of tectonics. This suggestion coincides with the conclusions of the studies of Siwalik and Brazeau-Paskapoo formations at their foreland basins (*35*).

The unconsolidated horizontally layered sequence of cyclothemic fluvial sediments of *tierra firme* are often discordantly located above slightly folded Tertiary sediments (Fig. 3) (*24, 33*). Campbell and Frailey (*7*) argue that the uppermost poorly consolidated layer is a result of early Holocene catastrophic floods following the melting of Andean glaciers or discharging of glacial lakes. This catastrophic flood period would have formed the most recent alluvium bed (the Iñapari Formation) (*36*), which would then be subject to species immigration from

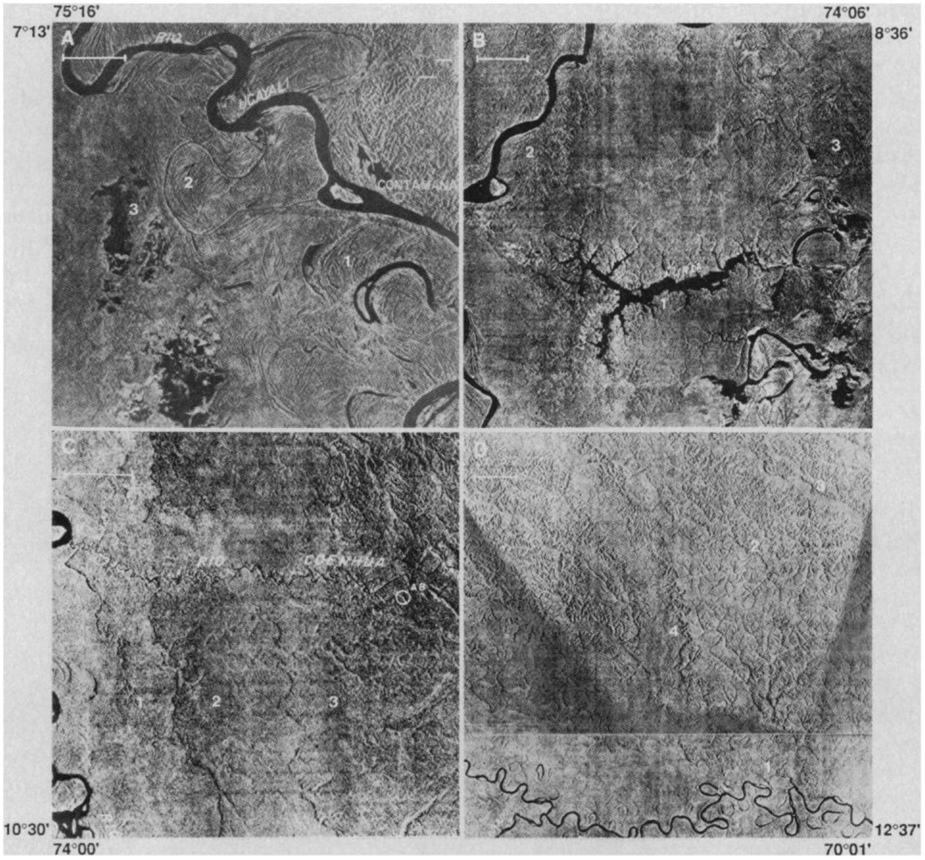

Fig. 2. Four areas with different geomorphic processes showing the geodynamic nature of western Amazonia (for locations, see Fig. 1). (**A**) Actively accumulating floodplain of River Ucayali with oxbow lakes (1), scroll bars (2), and wide depositionally downtrodden backswamp lakes (3) at the margins of the floodplains (elevation of the area about 140 m above sea level). (**B**) Tectonically or fluviodynamically (or both) isolated, old dissected terrace level with a *ria*-lake (1), surrounded by the present (2) and abandoned (3) floodplains of River Ucayali. The inundation of the *ria*-lake shows the tendency of the subsiding terrace level approaching the present level of floodplain sedimentation (~150 m). (**C**) The present (1) and terraced (2 and 3) floodplain generations, suggesting the relative emergence of the marginal areas in contrast to the central districts of the Ucayali basin (~220 m) (*28*). (**D**) Present (1) and fossil margins of abandoned floodplains (2 and 3) of River Madre de Díos with eroding secondary rivers. The series of fossil floodplain margins show the unidirectional lateral migration of the Madre de Díos floodplain toward the southwest caused by the tilting of the basement from northeast to southwest. Due to the inclination, the River Amigos (4) is cutting its channel through the former floodplain deposits of River Madre de Díos (~330 m). Sideways looking airborne radar (SLAR) imagery. Scale bars, 5 km.

the surrounding forest area.

We reject the catastrophic flood hypothesis because it neglects the actual mobile foreland character of the area (*14–16*) and gives no description of sedimentation processes differing from the present. There is also poor documentation of sufficient glacier formations in the Peruvian Andes (*37*). Rather, we interpret the uppermost fluvial beds as having been formed when laterally migrating Pleistocene-Holocene rivers, similar to present ones, have eroded the Tertiary sediments and aggraded their channel and floodplain deposits. Several investigators (*11, 24, 28*) suggest that this sequence of stratigraphy was initiated by tectonic uplift during the Plio-Pleistocene; the contact horizon between the Tertiary deposits and the uppermost poorly consolidated sediments with apparent cyclothems can only be observed in eroding river banks in areas of uplift. The discordance is probably of highly varying age in different areas.

The long history of fluvial perturbance and sedimentation in the western Amazonian ecosystem suggests that the ***várzea–tierra firme*** distinction is actually a time series from present to older alluvium beds (*38*). In central Amazonia, the uppermost ***tierra firme*** areas resemble those being currently deposited by the meandering and braided rivers at the Andean forelands (*11, 12*). This suggests that the same geodynamic processes that affect the modern biota of western Amazonia have been present with varying intensity in major parts of Amazonia during the Tertiary-Quaternary.

Current river dynamics have explanatory value with regard to the diversity maintenance processes of the Amazonian floodplain forests. The fluvial beds are a mosaic structure promoting edaphically differentiated communities which are of smaller size than the phytogeographic units of Amazonia (*39*). The argument that the unflooded ***tierra firme*** forest also grows widely over such a lithologic mosaic may be the key to understanding its floristic composition.

In western Amazonia, the uplifted older dissected areas (for example, East Perú–Acre and Napo) are separated by basinal areas with younger fluvial sediments. We suggest that biogeographic analyses based on age differences between these areas may reveal biological differences of the same type as have been proposed for the climatic refugia. In these cases the high endemism may be promoted by the older age of the areas and by possible isolation effects caused by gradational age differences on separating fluvial areas.

The shifting floodplain network may provide a speciation mechanism for the aquatic communities of upper Amazonia. All the major floodplains have several cases of channel alteration, which may have split aquatic populations during the Tertiary-Quaternary. The well-known high fish species diversity, especially in the Siluriformes, Cichlidae, and Characidae (*40*), may have its origin in shifting and splitting river systems. Besides splitting the populations, such channel alterations further mix the differentiated communities and may thus cause increase in within-habitat (α-type) diversity.

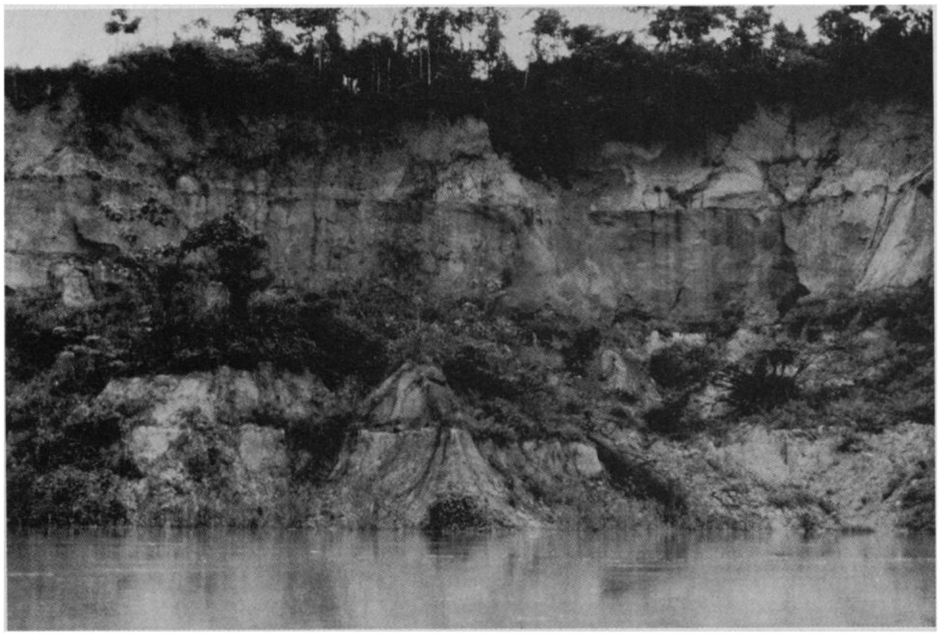

Fig. 3. A common stratigraphy of ***tierra firme*** levels in the western Amazonia with four horizontal fining upward cyclothems distinguished by slight horizontal discordancies. The stratigraphy is formed through sequential four-stage laterally and vertically aggrading floodplain sedimentation of meandering rivers. The channel and point bar deposits are well presented with minor presence of floodplain deposits. These sediments belong to the Madre de Díos or Iñapari Formations, the lower levels of which have recently been dated to late Pleistocene in age (36,500 before present) [sites are in southern Madre de Díos (*41*)]. The erosional discordance between upper poorly consolidated beds with cyclothems and older Tertiary deposits cannot be recognized at this location (~256 m). The site is located at 12°39′S and 69°09′W (River Tambopata).

REFERENCES AND NOTES

1. J. Haffer, *Science* **165**, 131 (1969).
2. G. T. Prance, Ed., *Biological Diversification in Tropics*, (Columbia Univ. Press, New York, 1982).
3. G. T. Prance, *Ann. Miss. Bot. Garden* **69**, 594 (1982).
4. E. Connor, *TREE* 1, 165 (1987); C. Schubert, *Interciencia* **11**, 278 (1986); G. Irion, *Trop. Ecol.* **23**, 76 (1982).
5. K.-b. Liu, and P. A. Colinvaux, *Nature* (*London*) **318**, 556 (1986).
6. J. Salo *et al.*, *ibid.* **322**, 254 (1986).
7. K. E. Campbell, Jr., and C. D. Frailey, *Natl. Geogr. Soc. Res. Rep. 189* (1977); *Quaternary Res.* **21**, 369 (1984); K. E. Campbell, Jr., C. D. Frailey, J. Arellano L., *Contrib. Sci.* **364**, 1 (1986).
8. P. A. Colinvaux *et al.*, *Nature* (*London*) **313**, 42 (1985).
9. *Tectonic Map of South America 1:5,000,000* (Departamanto National da Produçáo Mineral, Comission for the Geological Map of the World, Unesco, Brasília, 1978).
10. L. G. Weeks, *Bull. Am. Assoc., Petrol. Geol.* **31**, 1194 (1947).
11. Projeto RADAMBRASIL, "Levantamento de recursos naturais" (Ministerio das Minas e Energia, Rio de Janeiro, 1977), vol. 15.
12. *Geologia do Brasil* (Departamento Nacional da Produçáo Mineral, Brasília, 1984).
13. J. Guizado J., *Bol. Soc. Geol. Perú* **45**, 25 (1975); D. L. Browman, *Nature* (*London*) **302**, 568 (1983).
14. C. K. Ham and L. J. Herrera, Jr., *Am. Assoc. Petrol. Geol. Mem. 2* (1963), p. 47.
15. T. E. Jordan *et al.*, *Geol. Stud. Am. Bull.* **94**, 341 (1983); G. Suárez, P. Molnar, C. Burchfiel, *J. Geophys. Res.* **88**, 10403 (1983).
16. B. Dalmayrac, *Inst. Geol. Min. Metal. Bol. 11*, *Ser. D* (1986).
17. J. P. Morgan and W. G. McIntyre, *Bull. Geol. Soc. Am.* **70**, 319 (1959); J. M. Coleman, *Sed. Geol.* **3**, 129 (1969).
18. F. G. Huerta, *Bol. Soc. Geol. Perú* **62**, 125 (1979).
19. M. Martinez V., *ibid.* **67**, 85 (1980); L. Cánepa and F. R. Laura, *ibid.* **66**, 13 (1980).
20. W. F. Jenks, Ed., *Geol. Soc. Am. Mem.* **65** (1956); H. J. Harrington, *Bull. Am. Assoc. Petrol. Geol.* **46**, 1773 (1962).
21. F. Soto V., *Bol. Soc. Geol. Perú* **60**, 233 (1979).
22. G. Steinmann, Ed., *Geologie von Perú* (Carl Winters Universitets Buchhandlung, Heidelberg, 1933).
23. E. Koch and E. Blissenbach, *Bol. Soc. Geol. Perú* **39**, 7 (1962).
24. B. Kummel, *Bull. Geol. Soc. Am.* **59**, 1217 (1948).
25. M. D. Williams, *Soc. Geol. Perú* Volumen Jubilar (1949), part 2.
26. W. Rüegg and A. Rosenzweig, *ibid.*
27. A. I. Oliveira, *Geol. Soc. Am. Mem. 65* (1956), pp. 1–62.
28. E. Koch, *Bol. Soc. Geol. Perú* **34**, 32 (1959).
29. J. Guizado J., *Reunion Anual a Nivel de Expertos* (Petroperu, Lima, 1986), vol. 2.
30. W. Ruegg, *Petrol. Eng.* (30 April 1958).
31. V. R. Baker, *Can. Soc. Petr. Geol. Mem.* **5**, 211 (1978).
32. Mapa geologico del Perú. *Inst. Geol. Miner. Perú Bol. 28* (1977).
33. J. T. Singewald, *Bull. Geol. Soc. Am.* **39**, 447 (1928); P. W. Chase, *J. Geol.* **41**, 513 (1933); V. Oppenheim, *Bull. Am. Assoc. Petrol. Geol.* **21**, 97 (1937); *ibid.* **30**, 254 (1946); *Bol. Soc. Geol. Perú* **45**, 83 (1975); G. G. Simpson, *J. Paleontol.* **35**, 620 (1961); ______ and C. Paula Couto, *Iheringia, Sér. Geol. Porto Alegre* **6**, 11 (1981).

34. J. R. Beerbower, *State Geol. Surv. Kansas Bull.* **169**, 31 (1964).
35. J. R. McLean and T. Jerzykiewitcz, *Can. Soc. Petrol. Geol. Mem.* **5**, 441 (1978); L. B. Halstead and A. C. Nada., *Bull. Geol. Assoc.* **6**, 63 (1973).
36. ONERN, "Inventario, evaluación e integración de los recursos naturales de la zona de los Ríos Inambari y Madre de Díos" (Lima, 1972).
37. J. H. Mercer, in *Proceedings of the SASQUA International Symposium*, Balleema, Rotterdam, 1984, p. 45.
38. J. Salo and R. Kalliola, in *Rainforest Regeneration and Management*, J. Jeffers, Ed. (MAB Book Series, Unesco, Paris, in press.
39. A. Ducke and G. A. Black, *Anais. Acad. Bras. Cienc.* **25**, 1 (1953).
40. J. Gery, *Characoids of the World* (TFH-Publications, Neptune, NJ, 1977); S. H. Weitzman and M. Weitzman, in *Biological Diversification in Tropics*, G. T. Prance, Ed. (Columbia Univ. Press, New York, 1982), pp. 403–422.
41. K. E. Campbell, Jr. and L. Romero, in Proceeding *VI Congreso Peruano de Geologia, Resumenes* (Sociedad Geologica del Perú, Lima, 1987).
42. We thank W. Danjoy Arias, G. Glückert, E. Haukioja, V. Lappalainen, J. Lehtovaara, R. Neller, S. Neuvonen, P. Niemelä, M. Soikkeli, and T. Vuorisalo for their constructive comments, and colleagues at INGEMMET and Petroperu, Lima, for discussion. H. Venho and M. Valtonen assisted in figure processing. ONERN, Lima provided the SLAR material. Ministerio de Agricultura, Lima, provided logistic help for the work. Funded by FINNIDA and the Academy of Finland (contract 09/471).

5 May 1987; accepted 10 September 1987

Generation of a Hybrid Sequence-Specific Single-Stranded Deoxyribonuclease

D. R. COREY AND P. G. SCHULTZ*

The relatively nonspecific single-stranded deoxyribonuclease, staphylococcal nuclease, was selectively fused to an oligonucleotide binding site of defined sequence to generate a hybrid enzyme. A cysteine was substituted for Lys^{116} in the enzyme by oligonucleotide-directed mutagenesis and coupled to an oligonucleotide that contained a 3′-thiol. The resulting hybrid enzyme cleaved single-stranded DNA at sites adjacent to the oligonucleotide binding site.

ONE APPROACH TO DEVELOPING biological catalysts with tailored specificities involves redesigning existing enzyme active sites by the method of oligonucleotide-directed mutagenesis (*1*). Alternatively, entire binding or catalytic domains may be added or replaced to generate hybrid enzymes with novel specificities. We have applied this latter strategy to the construction of a sequence-specific single-stranded deoxyribonuclease (DNase) consisting of the relatively nonspecific enzyme, staphylococcal nuclease, selectively fused to an oligonucleotide binding site of defined sequence. The hybrid enzyme selectively cleaves single-stranded DNA adjacent to the oligonucleotide binding site. The hybrid hydrolyzes the phosphodiester bond of DNA (*2*), in contrast to existing chemical strategies for selectively cleaving DNA that result in degradation of the ribose backbone (*3–5*).

Staphylococcal nuclease is a well-characterized stable enzyme consisting of a single polypeptide chain 149 amino acids in length (*6–9*). The enzyme preferentially hydrolyzes the phosphodiester bonds of single-stranded RNA, single-stranded DNA, and duplex DNA at A,U- or A,T-rich regions to generate 3′-phosphate and 5′-hydroxyl termini (*10*); Ca^{2+} is required for enzymatic activity, providing a mechanism for modulating enzyme action (*6*). The structure and mechanism of staphylococcal nuclease have been elucidated from a series of chemical, physical, and genetic studies. An x-ray crystal structure of a staphylococcal nuclease–diphosphothymidine (pTp)–Ca^{2+} complex has been determined to 1.5 Å (Fig. 1) (*8, 11*). The pyrimidine ring of the inhibitor pTp fits into a hydrophobic pocket at the enzyme surface and the 5′-phosphate is near Arg^{35} and Arg^{87}. Glu^{43} is thought to act as a general base for activation of the attacking water molecule, whereas Arg^{35}, Arg^{87}, and Ca^{2+} stabilize the trigonal bipyramidal transition state (*11, 12*).

The geometry of the bound inhibitor pTp suggests that coupling of the 3′-terminus of an oligonucleotide binding domain to Lys^{116} on the enzyme surface should align a hybridized RNA or DNA substrate with the enzyme active site. A flexible tether was incorporated to allow some variability between the hybridized substrate and the active site residues. An oligomer 15 nucleotides (nt) in length, 5′-CCCGCACAAGCCG-CT-3′ (melting temperature, 62°C) (*13*), was coupled to staphylococcal nuclease by a disulfide exchange reaction. This coupling strategy required the introduction of a free thiol at both the 3′-terminus of the oligonucleotide and at residue 116 of the enzyme. Subsequent disulfide exchange should proceed under mild conditions and with high selectivity because of the absence of competing free thiols in DNA and staphylococcal nuclease.

We have adapted existing methods for the solid-phase phosphotriester or phosphoramidite synthesis of oligonucleotides to allow rapid incorporation of free 3′-thiols (*14*). The 3′-thiol is introduced in the form of a disulfide linkage between the 3′-nucleoside and the solid-phase support prior to the first step of oligonucleotide synthesis (Fig. 2). After synthesis and deprotection of the oligomer, the disulfide bond is cleaved and subsequently reacted with 2,2′-dithiodipyridine to afford the 3′-*S*-thiopyridyl oligonucleotide. This modified oligonucleotide has been demonstrated to selectively react in high yields under mild conditions with a thiol-containing fluorescent probe (*14*).

A free thiol was introduced into staphylococcal nuclease by replacement of Lys^{116}

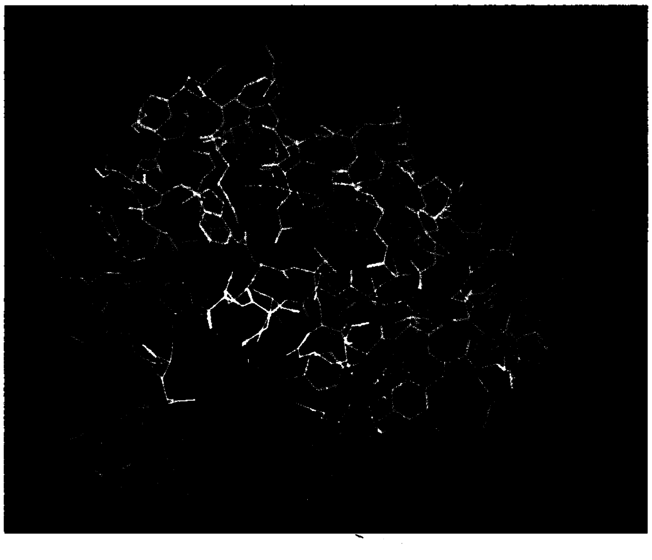

Fig. 1. X-ray crystal of a staphylococcal nuclease–pTp–Ca^{2+} complex (*11*). The active site residues Asp^{21}, Arg^{35}, Asp^{40}, Thr^{41}, Glu^{43}, and Arg^{87} are yellow, the inhibitor pTp is red, and Cys^{116} is green.

Department of Chemistry, University of California, Berkeley, CA 94720.

*To whom all correspondence should be addressed.